Reprinted from

JAPANESE JOURNAL OF
APPLIED
PHYSICS

RAPID COMMUNICATION

Extremely High Purcell Factor of Plasmonic Modes in Thin Nano-Metallic Cylinders

Jin-Kyu Yang

Jpn. J. Appl. Phys. **50** (2011) 060205

Japanese Journal of Applied Physics **50** (2011) 060205 **RAPID COMMUNICATION**
DOI: 10.1143/JJAP.50.060205

Extremely High Purcell Factor of Plasmonic Modes in Thin Nano-Metallic Cylinders

Jin-Kyu Yang*

Department of Optical Engineering, Kongju National University, Kongju, Chungnam 314-701, Korea

Received February 26, 2011; accepted March 17, 2011; published online June 6, 2011

We numerically study the ultrahigh Purcell factor ($>10^4$) of plasmonic modes in thin metallic nanodisk and nanoring structures by fully three-dimensional (3D) finite-difference time-domain (FDTD) simulation. Because of their extremely small mode volume ($\sim 10^{-5}\,\lambda_0{}^3$, λ_0 is the resonant wavelength in vacuum), plasmonic modes with a large radiative loss can have a high decay rate. Because of a uniform field enhancement inside their rings, nano-metallic ring structures show high potential for controlling high-extraction efficiency and single molecular sensing utilized in surface-enhanced Raman scattering. © 2011 The Japan Society of Applied Physics

Surface plasmon (SP) modes have attracted the interest of many researchers in the nano-optics field because of their extremely strong field confinement beyond the diffraction limit.[1,2] In recent years, various plasmonic devices based on SP modes, such as subwavelength lasers, compact waveguides, and biosensors, have been widely investigated because of their ultrasmall mode volume V and relatively high quality factor Q.[3–5] In particular, one of the major studies on SP phenomena is about the enhancement of spontaneous emission rate because of the strong ripple effect of SP modes in light-emitting devices.[6,7]

In general, the spontaneous emission rate is related to the Purcell factor, which is proportional to the ratio of the possible optical modes contributing to the desired radiation to the total optical modes at a given energy. The Purcell factor is expressed by

$$F = \frac{3Q}{4\pi^2 V}\left(\frac{\lambda}{n}\right)^3,$$

where λ is the resonant wavelength of the SP mode and n is the index of refraction of the host medium. In nanoscale metallic structures, despite their small Q factor due to the large radiation and ohmic losses of electron oscillations the Purcell factor is comparable to that of high-Q dielectric modes because of the extremely small mode volume beyond the diffraction limit.[8] However, because SP modes have hot spots on the surface of metals and exponentially decay along the host medium, coupled SP-mediated photoluminescence from light emitters could be suppressed by ohmic absorption. Therefore, one key issue in SP-assisted light extraction is finding a SP mode with a small ohmic loss and a high radiative decay rate. In this study, we numerically investigate SP modes and their Purcell factor in 3–5-nm-thick metallic structures by three-dimensional (3D) finite-difference time-domain (FDTD) simulation.

In the simulation, gold is modeled using the Drude equation from visible to infrared frequencies on the basis of the estimation of the data cited from refs. 9 and 10. To realize time-dependent dispersive loss in metals, the auxiliary differential equation method is adopted in 3D FDTD. In spatially digitized numerical simulation, the minimum spatial size (grid size) should be small enough to resolve the field distribution. In this study, a 1 nm resolution in space is maintained.

First, we consider a thin nano-metallic disk to reduce the ohmic loss of SP modes. Figure 1(a) shows a dipolar SP mode in a 5-nm-thick Au disk with a 60 nm radius. Here, the background material (host medium) is air. In this case, the Q factor is about 15 and the resonant wavelength is 860 nm. Note that the Q factor is estimated from the decay time of the SP mode by fitting the electric energy decay. The upper panel is a cut view of the electric field intensity at the center of the slab, and the lower panel is a cut view of the electric field intensity perpendicular to the slab. The electric field of the SP mode is strongly confined near the edge of the Au disk. Therefore, the mode volume $V = \int \varepsilon|E|^2\, d\tau / (\varepsilon|E|2)_{\max}$ is $\sim 0.000030\lambda_0{}^3$, where λ_0 is the resonant wavelength in vacuum, and the Purcell factor of the SP mode is about 37000, which is two orders of magnitude higher than that of the photonic crystal single defect mode.[11] Moreover, because of the low Q factor of the SP mode, it is possible to achieve both a high Purcell factor and a high decay rate in a wide spectral range simultaneously. However, the electric field intensity is strongly localized near the surface of Au and exponentially decays in the air; therefore, the ohmic loss increases. Thus, metal nanodisk structures are not good for SP-assisted light extraction devices.

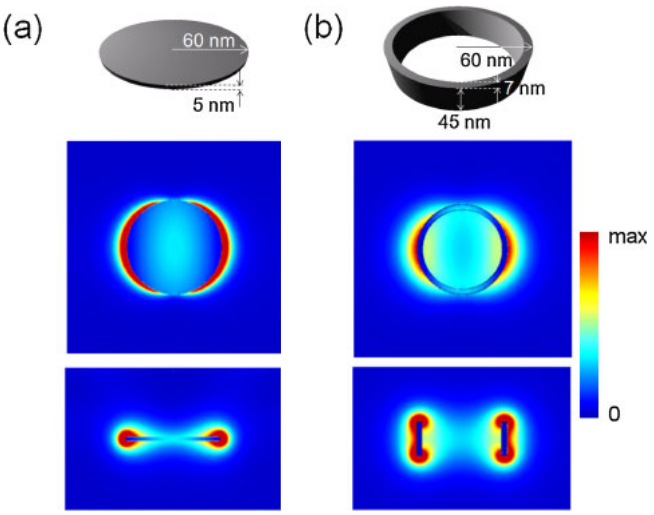

Fig. 1. (Color online) Dipolar SP modes in (a) 5-nm-thick Au disk with 60 nm radius and (b) 7-nm-thick Au ring with outer radius and height of 60 and 45 nm, respectively. The upper panel shows the electric field intensity distribution along the center of the slab, and the lower panel shows that perpendicular to the slab. The colored bar on the right indicates the intensity scale.

Figure 1(b) shows the electric field distribution of the dipolar SP mode in a 7-nm-thick Au ring where the outer radius and height are 60 and 45 nm, respectively. The Q

*E-mail address: jinkyuyang@kongju.ac.kr

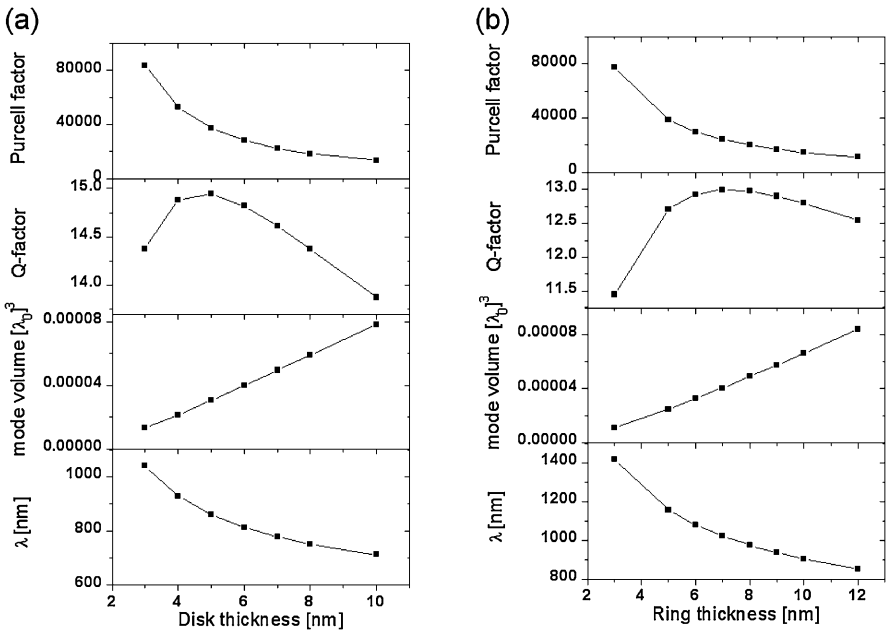

Fig. 2. Optical properties of (a) Au nanodisk and (b) Au nanoring as functions of disk thickness and ring width.

factor is 13 and the resonant wavelength is 1020 nm. The electric field intensity exponentially decays outside the Au ring. However, inside the ring, the electric field intensity is uniformly enhanced.[4] The mode volume is still extremely small at about $0.000040\lambda_0{}^3$; therefore, the Purcell factor is very high at about 24000. In comparison with the dipolar SP mode of the Au nanodisk, the mode volume increases by 33% and the Q factor decreases by 13%, while the physical metallic volume of the Au nanoring is twice that of the disk. Moreover, although the nanoring has a surface area that is 2.6 times larger than that of the disk, the Purcell factor of the nanoring is only 35% lower than that of the nanodisk. This implies that the metal nanoring structure is efficient for obtaining a high Purcell factor with a high decay rate in spite of the relatively large metallic volume and surface compared with the nanodisk.

To study the effects of metallic volume on the optical properties of the SP mode, the mode volume, Q factor, and Purcell factor are investigated as functions of the thickness of the nanostructures. Figure 2(a) shows the optical properties of dipolar SP modes in the Au nanodisk whose thickness varies from 3 to 10 nm. The radius of the Au disk and the refractive index of the background material are fixed at 60 nm and 1.0, respectively. When the disk becomes thinner, the resonant wavelength increases and the mode volume decreases. Generally, when the wavelength is red-shifted, the ohmic loss in the metal decreases. However, the radiation loss increases owing to the reduced thickness. Therefore, the Q factor is maximized at a certain balanced point between radiation and absorption losses when the thickness changes. Here, the Q factor is maximized at approximately 15 at a thickness $d = 5$ nm. Because the change in the Q factor is not significant, the Purcell factor is inversely proportional to the mode volume. If the thickness of the nanodisk is smaller than 10 nm, the Purcell factor of the SP mode is greater by four orders of magnitude, which is extremely larger than that of a single-defect photonic crystal cavity.[11] Figure 2(b) shows the optical properties of the dipolar SP mode in a Au nanoring whose width varies from 3 to 12 nm. Here, the outer radius and height of rings are fixed at 60 and 45 nm, respectively. The mode volume and Q factor are very similar to those of a nanodisk even though the surface and volume of the metal are twice larger than those of the disk. Therefore, the Purcell factor is still greater by four orders of magnitude when the width of the ring is smaller than 12 nm. From this result, we expect that the metal nanoring is a more promising structure for spontaneous emission enhancement owing to not only the Purcell factor but also the uniform field enhancement inside the metal ring.

For the quantitative estimation of loss management in the SP mode in the Au nanoring structure, the Q factor is calculated when the material loss is changed. The loss is inversely proportional to the Q factor. Therefore, the total loss could be simply expressed by $1/Q_{\mathrm{tot}} = 1/Q_{\mathrm{A}} + 1/Q_{\mathrm{R}}$. Here, $1/Q_{\mathrm{tot}}$ is the total loss, $1/Q_{\mathrm{A}}$ is the absorption loss, and $1/Q_{\mathrm{R}}$ is the radiation loss. As previously mentioned, the ohmic loss of gold is realized in FDTD simulation using the Drude model, where the dielectric constant is expressed by

$$\varepsilon_{\mathrm{D}}(\omega) = \varepsilon_{\mathrm{D}}(\infty) - \frac{\omega_{\mathrm{D}}^2}{\omega(\omega - i\Gamma_{\mathrm{D}})}.$$

Here, the plasma frequency ω_{D} is $1.453 \times 10^{16}\ \mathrm{s}^{-1}$ and the electron–neutral collision frequency Γ_{D} is $1.109 \times 10^{14}\ \mathrm{s}^{-1}$ in gold at room temperature from 650 to 1250 nm.[10] According to the free-electron model of metals, absorption loss is related to collision frequency, which decreases with decreasing temperature.[12,13] From the reference electric resistivity of gold,[14] we scaled Γ_{D} as a function of temperature. Figure 3 shows the temperature dependences of the resonant wavelength of the SP mode and its total Q factor. When the temperature changes from 560 to 0 K, the resonant wavelength only changes by less than 0.4%. This implies that the field distribution of the resonant mode does not change, so the radiation properties are almost the same. Because the ohmic loss disappears at zero temperature, the total loss is only due to the radiation loss, which corresponds to $Q_{\mathrm{R}} \sim 60$. From

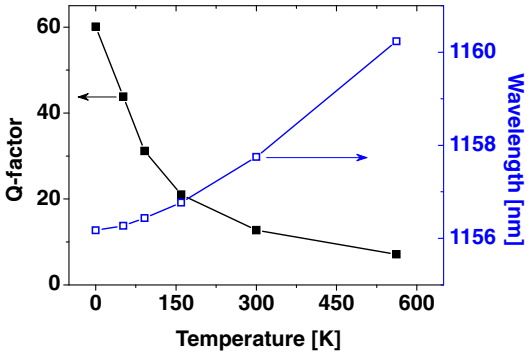

Fig. 3. (Color online) Temperature dependences of Q factor and resonant wavelength of dipolar SP mode in Au nanoring.

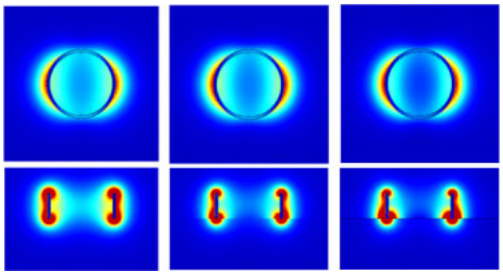

Fig. 4. (Color online) Electric field intensity distributions of Dipolar SP modes in Au nanoring on top of different dielectric substrates. The left panel is in air, the center panel is on a glass substrate ($n = 1.5$), and the right panel is on a Si substrate ($n = 3.4$).

$Q_{tot} \sim 13$ at room temperature, Q_R and Q_A are estimated to be about 60 and 17, respectively. Hence, the absorption decay rate is still 3.6 times higher than the radiation decay rate in the Au nanoring structure at room temperature. We also checked the change in the Purcell factor when the height of the Au nanoring varies from 10 to 60 nm. If the height decreases, the mode volume decreases and the Purcell factor increases further. In particular, the Q factor is maximized by around 15 when the height is 30 nm. When the height decreases until 10 nm, the Purcell factor increases further by 3×10^5. However, the resonant wavelength also increases by 1600 nm. Therefore, it is necessary to scale the nanoring geometry to match the resonant wavelength with a target wavelength.

In a realistic case, a nanoring on top of a dielectric substrate is considered. Figure 4 shows the electric field intensities. The upper panel is a cut view of the electric field intensity at the center of the slab, and the lower panel is a cut view of the electric field intensity perpendicular to the slab. In the case of the Au nanoring on top of the glass substrate ($n = 1.5$), the electric field intensity distribution is shown at the center of Fig. 4. When the index increases further ($n = 3.4$), the field becomes more concentrated at the boundary between the air and the substrate, as shown in the right panel of Fig. 4. The electric field intensity inside the nanoring decreases as the index increases because of the strong confinement of the field near the substrate, but it remains enhanced. As the index increases, the resonant wavelength is red-shifted because of the enhanced confinement of light near the air-substrate boundary, and the Q factor decreases owing to the increasing radiation loss caused by symmetry breaking induced by the substrate. Generally, the ohmic loss decreases when the wavelength increases. Therefore, decreasing the Q_R factor of the dielectric substrate with a high index of refraction is more significant than decreasing the Q_{tot} factor. Moreover, in consideration of energy transferring from the active layer inside the substrate, the strong concentration at the boundary between the metal and the substrate is good to extract the light from the emitter. From this result, we expect that metal nanorings on top of a dielectric substrate with a high index of refraction will be more efficient for SP-assisted light extraction.

One promising application of highly confined light in the dipolar SP mode is to single-molecule detection based on surface-enhanced Raman scattering (SERS).[15,16] In general, the enhancement of the Raman cross section is proportional to the power ratio squared between the local electric intensity and the input electric intensity expressed by $R = |E_{loc}|^4/|E_{in}|^4$. From Maeir's paper,[2] the SERS cross-sectional enhancement can be expressed using the resonant mode amplitude

$$\sqrt{R} = \frac{\sigma_{rad}}{4\pi^2 c^2 \eta \varepsilon_0 \lambda_0}\left(\frac{Q}{Q_{rad}}\right)\left(\frac{Q}{V_{eff}}\right),$$

where σ_{rad} is the effective radiation cross section and η is the impedance of free space. Generally, when metal nanoparticles become smaller, the Q factor of SP modes decreases. However, the decrease in V_{eff} is much faster than the increase in the Q factor; therefore, Q/V_{eff} is extremely large. In the Au nanoring structure with a 7 nm width and a 45 nm height, Q/V_{eff} is about $3 \times 10^5\,\lambda_0{}^3$; thus, $R \sim 10^{11}$, which is similar to that of two Ag nanoparticles separated by 3–5 nm.[17]

In summary, we numerically investigate the optical properties of dipolar SP modes in 3–5-nm-thick Au nanodisks and nanorings by 3D FDTD simulation. Because of the extremely small mode volume ($\sim 10^{-5}\,\lambda_0{}^3$), an ultrahigh Purcell factor ($>10^4$) is achieved in thin metallic nanodisk and nanoring structures. Because of the uniform field enhancement inside their rings, Au nanoring structures are a good candidate for controlling high extraction efficiency and single molecular sensing utilizing SERS.

Acknowledgement This work was supported by the KOSEF through OPERA (R11-2003-022).

1) W. L. Barnes *et al.*: Nature **424** (2003) 824.
2) S. A. Maier: Opt. Express **14** (2006) 1957.
3) R. F. Oulton *et al.*: Nature **461** (2009) 629.
4) J. Aizpurua *et al.*: Phys. Rev. Lett. **90** (2003) 057401.
5) J. Homola *et al.*: Sens. Actuators B **54** (1999) 3.
6) J. Vuckovic *et al.*: IEEE J. Quantum Electron. **36** (2000) 1131.
7) K. Okamoto *et al.*: Nat. Mater. **3** (2004) 601.
8) J. Gerard and B. Gayral: J. Lightwave Technol. **17** (1999) 2089.
9) J. K. Yang *et al.*: Opt. Express **16** (2008) 1951.
10) D. W. Lynch and W. R. Hunter: in *Handbook of Optical Constants of Solids*, ed. E. D. Palik (Academic, Orlando, FL, 1985) Vol. 1, p. 350.
11) H. G. Park *et al.*: Science **305** (2004) 1444.
12) M. T. Hill *et al.*: Nat. Photonics **1** (2007) 589.
13) S. H. Kwon *et al.*: Nano Lett. **10** (2010) 3679.
14) R. A. Matula: J. Phys. Chem. Ref. Data **8** (1979) 1147.
15) K. Kneipp *et al.*: Phys. Rev. Lett. **78** (1997) 1667.
16) S. Nie and S. R. Emory: Science **275** (1997) 1102.
17) E. Hao and G. C. Schatz: J. Chem. Phys. **120** (2004) 357.